ORIGINAL RESEARCH

Deletion of c-FLIP from CD11b^{hi} Macrophages Prevents Development of Bleomycin-induced Lung Fibrosis

Alexandra L. McCubbrey[1,2], Lea Barthel[2], Michael P. Mohning[1,2], Elizabeth F. Redente[1,3,4], Kara J. Mould[1], Stacey M. Thomas[2], Sonia M. Leach[5,6], Thomas Danhorn[5,6], Sophie L. Gibbings[3], Claudia V. Jakubzick[3,7], Peter M. Henson[3], and William J. Janssen[1,2]

[1]Division of Pulmonary Diseases and Critical Care Medicine, Department of Medicine, University of Colorado Denver School of Medicine, Aurora, Colorado; [2]Division of Pulmonary, Critical Care, and Sleep Medicine, Department of Medicine, and [3]Program in Cell Biology, Department of Pediatrics, National Jewish Health, Denver, Colorado; [4]Department of Research, Veterans Affairs Eastern Colorado Health Care System, Denver, Colorado; [5]Center for Genes, Environment, and Health, and [6]Department of Biomedical Research, National Jewish Health, Denver, Colorado; and [7]Integrated Department of Immunology, National Jewish Health and University of Colorado Denver Anshutz Campus, Denver, Colorado

ORCID ID: 0000-0002-2049-9609 (A.L.M.).

Abstract

Idiopathic pulmonary fibrosis is a progressive lung disease with complex pathophysiology and fatal prognosis. Macrophages (MΦ) contribute to the development of lung fibrosis; however, the underlying mechanisms and specific MΦ subsets involved remain unclear. During lung injury, two subsets of lung MΦ coexist: Siglec-F^{hi} resident alveolar MΦ and a mixed population of CD11b^{hi} MΦ that primarily mature from immigrating monocytes. Using a novel inducible transgenic system driven by a fragment of the human CD68 promoter, we targeted deletion of the antiapoptotic protein cellular FADD-like IL-1β–converting enzyme–inhibitory protein (c-FLIP) to CD11b^{hi} MΦ. Upon loss of c-FLIP, CD11b^{hi} MΦ became susceptible to cell death. Using this system, we were able to show that eliminating CD11b^{hi} MΦ present 7–14 days after bleomycin injury was sufficient to protect mice from fibrosis. RNA-seq analysis of lung MΦ present during this time showed that CD11b^{hi} MΦ, but not Siglec-F^{hi} MΦ, expressed high levels of profibrotic chemokines and growth factors. Human MΦ from patients with idiopathic pulmonary fibrosis expressed many of the same profibrotic chemokines identified in murine CD11b^{hi} MΦ. Elimination of monocyte-derived MΦ may help in the treatment of fibrosis. We identify c-FLIP and the associated extrinsic cell death program as a potential pathway through which these profibrotic MΦ may be pharmacologically targeted.

Keywords: macrophage; fibrosis; c-FLIP; RNA-seq; IPF

Clinical Relevance

Pulmonary fibrosis is a progressive, deadly disease of unclear etiology; understanding the underlying mechanisms is critical for developing effective treatments. We have identified a specific subpopulation of mainly monocyte-derived macrophages that drive the development of fibrosis and have described their unique profibrotic signature using RNA-seq. Removing this population abrogates the development of fibrosis.

(Received in original form April 14, 2017; accepted in final form August 16, 2017)

This work was supported by National Institutes of Health (NIH) grants R01HL109517 (W.J.J.), NIH R01HL114381 (W.J.J. and P.M.H.), NIH F32 HL131397-01 (K.J.M.), NIH F32 HL126333 (M.P.M.), VA-CDA2 1IK2BX002401-01A2 (E.F.R.), NIH T32 HL007085-42 (A.L.M.); the Cancer Center Flow Cytometry Shared Resource at the University of Colorado–Anschutz Medical Campus is supported by National Cancer Institute (NCI) P30CA046934.

Author Contributions: A.L.M. performed research, analyzed data, and wrote the manuscript; L.B., M.P.M., and E.F.R. performed research and contributed to the manuscript; K.J.M., S.M.T., S.L.G., and C.V.J. contributed to the manuscript; S.M.L. and T.D. performed the bioinformatics and contributed to the manuscript; P.M.H. contributed to the manuscript and the conceptual design of the study; W.J.J. designed the research, analyzed data, and wrote the manuscript.

Correspondence and requests for reprints should be addressed to Alexandra L. McCubbrey, Ph.D., University of Colorado–Anschutz Medical Campus, 1300 19th Avenue East, Aurora, CO 80045. E-mail: mccubbreya@njhealth.org.

This article has a data supplement, which is accessible from this issue's table of contents at www.atsjournals.org

Am J Respir Cell Mol Biol Vol 58, Iss 1, pp 66–78, Jan 2018

Originally Published in Press as DOI: 10.1165/rcmb.2017-0154OC on August 29, 2017
Internet address: www.atsjournals.org

Macrophages (MΦ) are known to be involved in fibrogenesis. Lung MΦ numbers are elevated both in patients with idiopathic pulmonary fibrosis (IPF), a progressive lung disease with complex pathophysiology and fatal prognosis (1, 2), and in murine models of pulmonary fibrosis (3, 4). However, the mechanisms by which MΦ impact fibrosis are unclear. The objectives of this study were to determine the roles played by MΦ subsets in the development of lung fibrosis and to determine if fibrosis could be attenuated by promoting MΦ apoptosis.

During homeostasis, there are two main types of MΦ in the murine lung: resident Siglec-F^{hi}CD11b^{lo} MΦ that reside in the alveolar space, and CD11b^{hi}Siglec-F^{lo} MΦ that occupy the lung interstitium. Siglec-F^{hi} MΦ (often called resident alveolar MΦ and highly expressing CD11c) arise during embryogenesis, populate the airspaces immediately after birth, and self-renew throughout life without replacement from circulating monocytes (5–9). CD11b^{hi} MΦ (often called interstitial MΦ [IMs]) also arise during embryogenesis, but are restricted to the lung interstitium and found in much lower numbers than Siglec-F^{hi} alveolar MΦ (5, 6).

After lung injury, MΦ numbers expand in both the alveolar and interstitial compartments. Studies using lung-shielded bone marrow chimeras, targeted MΦ or monocyte depletion, and CCR2$^{-/-}$ mice all suggest that monocytes recruited from the circulation are the dominant source of new MΦ (often termed *recruited* MΦ) after injury (10–12). Much like homeostatic resident IMs, newly recruited MΦ express high levels of CD11b and low levels of Siglec-F. Accordingly, during acute inflammation, three main MΦ populations exist in the lung. These include two types of resident MΦ (Siglec-F^{hi} CD11b^{lo} alveolar MΦ and CD11b^{hi}SiglecF^{lo} IMs), present before onset of inflammation and that remain throughout its course, and a third population of recruited MΦ in the alveolus and interstitium (also CD11b^{hi}SiglecF^{lo}) that derive from monocytes and are only present in the context of disease.

Studies that separate MΦ subsets are imperative for clarifying their roles in fibrogenesis (13). However, a lack of tools for distinguishing and manipulating MΦ subsets had previously hampered this objective. The identification of reliable cell surface markers that distinguish resident alveolar MΦ from other subtypes constitutes a recent advance (7, 10, 14, 15). In addition, we have developed a new transgenic system to target MΦ subsets (16). Whereas traditional drivers of *cre recombinase* (cre) constitutively affect all lung MΦ starting early in development, we recently described a system in which CD11b^{hi} MΦ can be selectively targeted in a time-dependent fashion. Targeting is achieved using a fragment of the human CD68 promoter coupled with the reverse tetracycline-controlled transactivator (hCD68rtTA). Administration of doxycycline to these animals rapidly activates tetracycline-responsive elements in CD11b^{hi} IMs and recruited MΦ. Siglec-F^{hi} MΦ are not affected (16). As described subsequently here, we leveraged this new method to selectively manipulate the survival of CD11b^{hi} MΦ during bleomycin-induced lung injury and test their contribution to fibrogenesis.

Appropriately timed apoptosis of lung MΦ is beneficial for resolution of inflammation and effective tissue repair. MΦ resistance to apoptosis is implicated in the development of murine fibrosis and human IPF (17). We have previously demonstrated that CD11b^{hi} MΦ are recruited to the alveolar space during LPS-induced lung injury, but disappear within 2 weeks as a consequence of cell surface Fas receptor (Fas)-FasL-mediated cell death (10). In comparison, MΦ numbers remain elevated for over 6 weeks after bleomycin-induced lung injury and fibrosis. Eventual decline in MΦ number correlates with resolution of fibrosis (4). Treatment of mice with TNF-α after bleomycin injury accelerates MΦ decline and hastens the resolution of fibrosis (4).

FasL and TNF-α both activate the extrinsic cell death pathway. To induce cell death, this pathway requires the simultaneous presence of a death-inducing ligand, expression of the corresponding death receptor, and a permissive intracellular environment. Ligation of FasL or TNF-α to their cognate surface receptors triggers the transproteolytic cleavage of pro–caspase-8 homodimers to active caspase-8. Whereas low levels of active caspase-8 activate NF-κB and promote survival, higher levels trigger programmed cell death (18, 19). Cellular FADD-like IL-1β–converting enzyme–inhibitory protein (c-FLIP) is a critical death effector domain–containing protein that restricts caspase-8 activation (20–23). Accordingly, loss of c-FLIP sensitizes murine and human MΦ to cell death (24–26).

We hypothesized that deleting c-FLIP in CD11b^{hi} MΦ would promote their death and attenuate the development of fibrosis. We crossed hCD68rtTA mice with tet-On-Cre and cFLIP$^{fl/fl}$ mice to create animals in which c-FLIP could be conditionally deleted in CD11b^{hi} IMs and recruited MΦ upon administration of doxycycline. Deletion of c-FLIP sensitized MΦ to programmed cell death and specifically reduced CD11b^{hi} MΦ numbers in the lungs. Moreover, deletion of c-FLIP in CD11b^{hi} MΦ at both early (Day 1) and delayed (Day 7) time points significantly attenuated the development of fibrosis. Finally, using improved surface marker identification (7), we assessed the transcriptome of CD11b^{hi} MΦ during bleomycin injury to identify potential mediators of their profibrotic function.

Methods

Animals

This study was approved and performed in accordance with the ethics guidelines of the Institutional Animal Care and Use Committee at National Jewish Health. cFLIP$^{fl/fl}$ mice (27) were provided by Dr. You-Wen He (Duke University, Durham, NC). Details on other strains are provided in the data supplement.

Bleomycin Injury

Bleomycin (TEVA Pharmaceuticals) was administered in a dose of 3 U/kg, adjusted for the weight of the mouse, in 50 μl of PBS. Bleomycin was instilled intratracheally using a modified gavage needle. Mice were sedated with isoflurane (Baxter) before intratracheal instillations.

Flow Cytometry

Cells were stained with surface antibody panels to identify myeloid populations and analyzed using an LSRII flow cytometer (BD) and FlowJo software (Tree Star) or sorted using Moflo XDP-100 with Summit v5.1 software (Beckman Coulter, Dako). Details can be found in the data supplement.

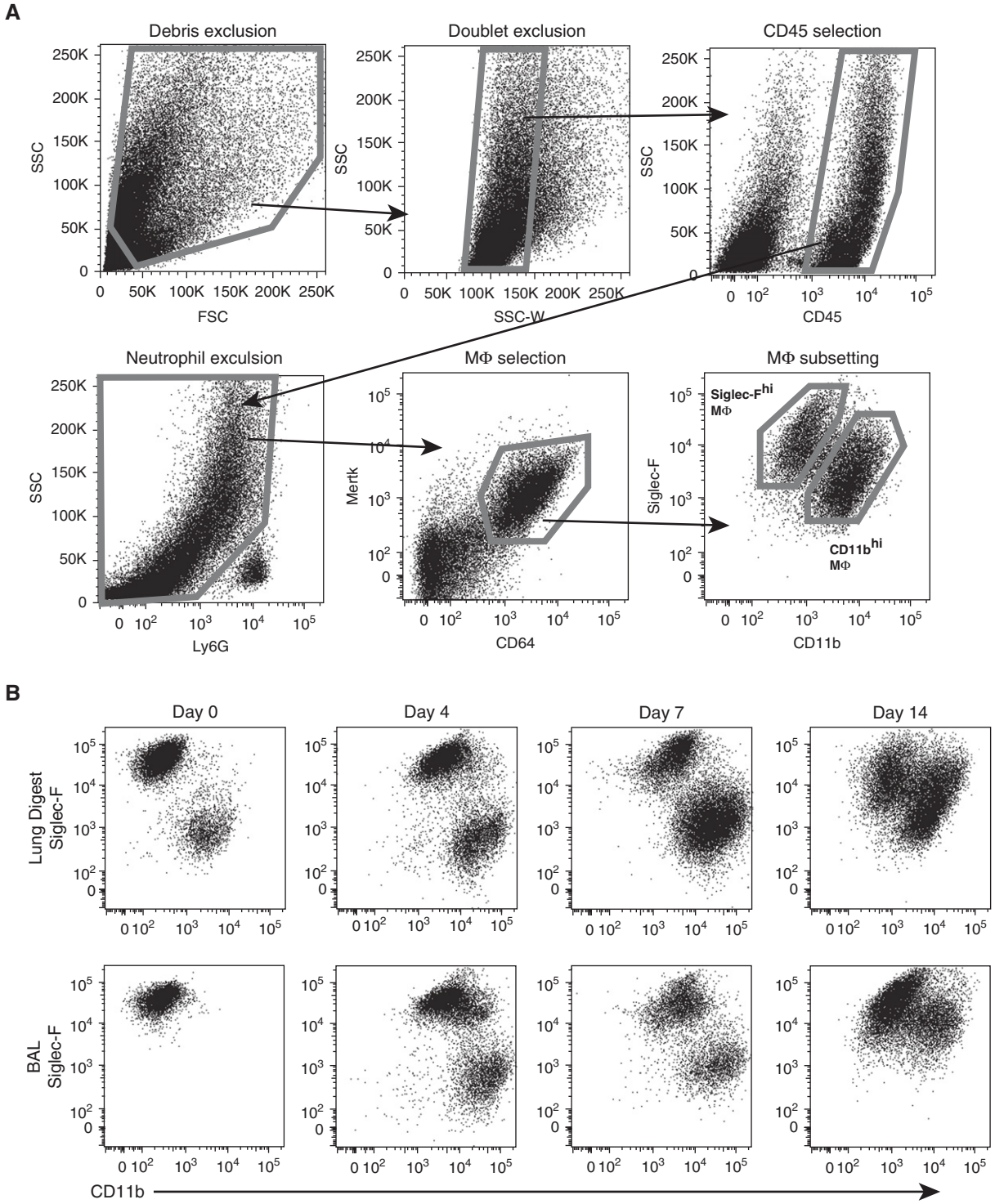

Figure 1. CD11b^{hi} macrophages (MΦ) drive an increase in total lung MΦ numbers after bleomycin. (*A*) Flow cytometry gating strategy used on lung digest and BAL to isolate Siglec-F^{hi} and CD11b^{hi} MΦ. Representative gating is shown on lung digest 14 days after bleomycin. Live cells are selected using size (forward scatter [FSC]) and granularity (side scatter [SSC]), doublets are excluded, and leukocytes are selected using CD45. Ly6G^{+} neutrophils are excluded, and CD64 and Mertk coexpression is used to select MΦ. (*B*) Siglec-F and CD11b are used to divide MΦ into two subpopulations. Representative dot plots from lung digest 4, 7, and 14 days after bleomycin are shown. (*C* and *D*) Total numbers of Siglec-F^{hi} and CD11b^{hi} MΦ were assessed in naive mice and mice 7 and 14 days after bleomycin. (*C*) MΦ in lung digest. (*D*) MΦ in BAL. Data from $n = 3$–5 mice/group shown as mean (±SEM). $^{**}P < 0.01$, $^{***}P < 0.001$. IT = intratracheal.

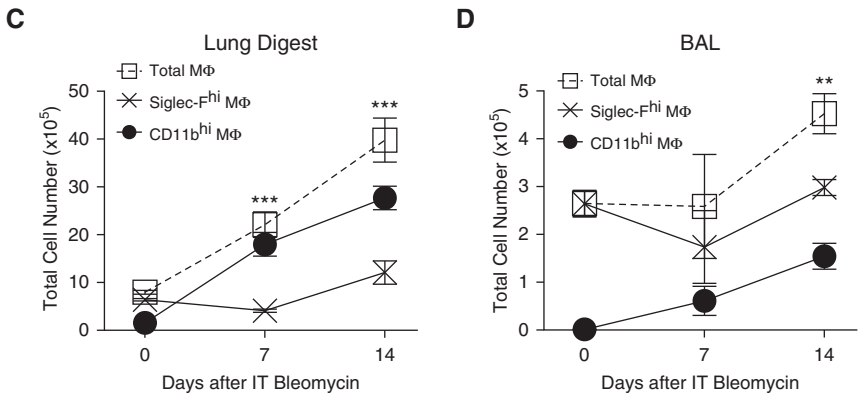

Figure 1. (Continued).

Measures of Caspase Activation

Cells recovered from BAL 7 days after bleomycin were adhesion purified to select for MΦ. Caspase-Glo (Promega, Madison, WI) assays were used per the manufacturer's instructions to measure caspase activity. Details can be found in the data supplement.

Assessing Fibrosis

Immediately after death, static compliance, a measurement that reflects the static elastic recoil pressure of the lungs at a volume of 0.95 ml, was determined using flexiVent (SCIREQ). Lungs were perfused with PBS and the right lung was saved for hydroxyproline analysis (28), or lungs were inflated with low-melt agarose, fixed in 10% formalin overnight, then paraffin embedded; 10-μm slices were stained with Trichrome and imaged with an Aperio system (Leica Biosystems).

RNA Isolation and RT-PCR

RNA was isolated from MΦ using the RNeasy micro kit (Qiagen) and DNase treated as instructed by the manufacturer. RNA was then processed for RNA-seq or RNA was reverse transcribed to cDNA using Superscript IV VILO Master Mix (Invitrogen) per the manufacturer's instructions for RT-PCR. Primer sequences in can be found in the data supplement.

RNA-Seq

Isolated total RNA from sorted cells was processed for next-generation sequencing library construction as developed in the NJH Genomics Facility for analysis with a Life Technologies Ion Proton next-generation sequencing platform. Details can be found in the data supplement.

Gene Expression Omnibus Data Sets

Microarray data from human MΦ (29) were obtained from the Gene Expression Omnibus (GEO; GEO accession no. GSE49072). Details can be found in the data supplement.

Statistical Analysis

Statistics for RNA-seq and GEO DataSet analyses were performed as described in the data supplement. For all other experiments, differences between two groups were examined using Student's unpaired *t* test. Differences among three or more groups were examined using ANOVA with Holm-Bonferroni's multiple comparison test *post hoc* analysis. A *P* value less than 0.05 was considered significant.

Results

CD11b^{hi} MΦ Account for the Increase in Total Lung MΦ after Bleomycin

MΦ contribute to lung fibrosis; however, the discrete contributions of MΦ subsets remain unclear. To develop a framework for studying the MΦ subsets, we first quantified MΦ during the initiation of fibrosis. We measured CD11b^{hi} MΦ and Siglec-F^{hi} MΦ in BAL fluid and enzymatically digested lungs from bleomycin-treated mice, adapting previously published protocols (7, 10, 14, 15) (Figure 1A). For all subsets, MΦ were identified based on their coexpression of CD64 and MER proto-oncogene tyrosine kinase (Mertk), cell surface molecules that, together, are specific for MΦ (30, 31). Notably, Ly6C^{hi} "inflammatory" monocytes express low CD64 and negligible Mertk, and were thus excluded by our MΦ gating strategy (*see* Figures E1A and E1B in the data supplement). High expression of Siglec-F was recently identified as a marker of resident alveolar MΦ (7), and use of Siglec-F and CD11b was sufficient to distinguish MΦ subpopulations in the lung at all time points (Figure 1B). In contrast, use of CD11b in conjunction with other markers failed to clearly separate CD11b^{hi} MΦ as inflammation progressed (Figures E1C and E1D). MΦ were examined in the first 2 weeks after injury, when fibrogenesis begins (4). Quantification of lung MΦ subsets revealed that CD11b^{hi} MΦ were responsible for the increase in MΦ numbers in both the airspace and tissue compartments (Figures 1C and 1D).

CD11b^{hi} MΦ Are Sensitized for Caspase-8–Dependent Cell Death after Deletion of c-FLIP

To specifically induce death of CD11b^{hi} MΦ and block their accumulation, we conditionally deleted c-FLIP (gene *cflar*) using our newly described hCD68rtTA system (16). c-FLIP is a nonenzymatic caspase-8 homolog that dimerizes with caspase-8 and inhibits its proapoptotic activity. By crossing hCD68rtTA with tet-On-Cre and cFLIP$^{fl/fl}$ mice, we were able to generate triple-transgenic mice in which administration of doxycycline leads to inducible deletion of *cflar* in CD11b^{hi} IMs and recruited MΦ (but not Siglec-F^{hi} resident alveolar MΦ). For simplicity, we designated these animals as cFLIP$^{\Delta/\Delta}$. In comparison, control mice (designated cFLIP$^{fl/fl}$) were littermates possessing floxed *cflar* and tet-On-Cre, but lacking hCD68rtTA (Figure E2A). To validate this system, cFLIP$^{\Delta/\Delta}$ and cFLIP$^{fl/fl}$ mice were treated with bleomycin, but doxycycline was withheld. BAL MΦ were harvested 7 days later and doxycycline was added *in vitro*. Doxycycline led to the loss of *cflar* expression in MΦ from cFLIP$^{\Delta/\Delta}$ mice; *cflar* was not deleted in MΦ from cFLIP$^{fl/fl}$ animals (Figure E2B). c-FLIP deletion alone did not induce obvious spontaneous death of cultured MΦ.

We next sought, in *ex vivo* studies, to determine the effect of c-FLIP deletion on MΦ sensitivity to cell death by assessing quantitative changes in the activity of

caspase-8 (initiator caspase in extrinsic cell death) and caspase-3 (downstream terminal executioner caspase). We also examined phenotypic changes associated with cell death: loss of plasma membrane integrity and loss of cell adherence. In brief, cFLIP$^{\Delta/\Delta}$ mice and cFLIP$^{fl/fl}$ littermate controls were treated with bleomycin, and BAL MΦ were isolated 7 days later and placed in culture. Doxycycline was added to delete c-FLIP and an activating α-Fas antibody was added to trigger the extrinsic cell death pathway. We deliberately chose a dose of α-Fas that triggered minimal Fas activation. The caspase-8 inhibitor, Z-IETD-FMK, was added to some wells as a negative control. As shown in Figure 2A, when doxycycline or α-Fas alone was added to cFLIP$^{\Delta/\Delta}$ MΦ there was no significant increase in caspase-8 activity. However, when α-Fas was added after doxycycline, caspase-8 activation increased. As anticipated, Z-IETD-FMK blocked this effect. Importantly, MΦ from littermate control mice (cFLIP$^{fl/fl}$) treated in parallel showed caspase-8 activity in response to α-Fas, but no additional effect of doxycycline (Figure 2B). Taken as a whole, these data demonstrate that death receptor ligation induces enhanced activation of caspase-8 when c-FLIP is deleted in lung MΦ.

To determine whether c-FLIP deletion would lead to downstream activation of caspase-3, *ex vivo* studies were repeated, again using BAL MΦ from bleomycin-treated cFLIP$^{\Delta/\Delta}$ and cFLIP$^{fl/fl}$ mice. Caspase-3 activity showed the same pattern as caspase-8 activity. Cotreatment with doxycycline (to delete c-FLIP) and the α-Fas significantly enhanced caspase-3 activation (Figure 2C), whereas c-FLIP deletion alone did not. Moreover, blocking caspase-8 with the inhibitor, Z-IETD-FMK, prevented caspase-3 activation, confirming that caspase-3 activation was downstream of caspase-8 activity (Figure 2C). MΦ from cFLIP$^{fl/fl}$ littermate control mice did not respond to doxycycline (Figure 2D).

Loss of plasma membrane integrity was observed in cFLIP$^{\Delta/\Delta}$ MΦ cotreated with doxycycline and α-Fas, but not in MΦ treated with α-Fas alone or in cFLIP$^{fl/fl}$ MΦ, providing additional evidence that c-FLIP deletion enables MΦ extrinsic cell death (Figure E2C). Leaving cFLIP$^{\Delta/\Delta}$ MΦ in culture for more than 12 hours after addition of α-Fas resulted in decreased cell

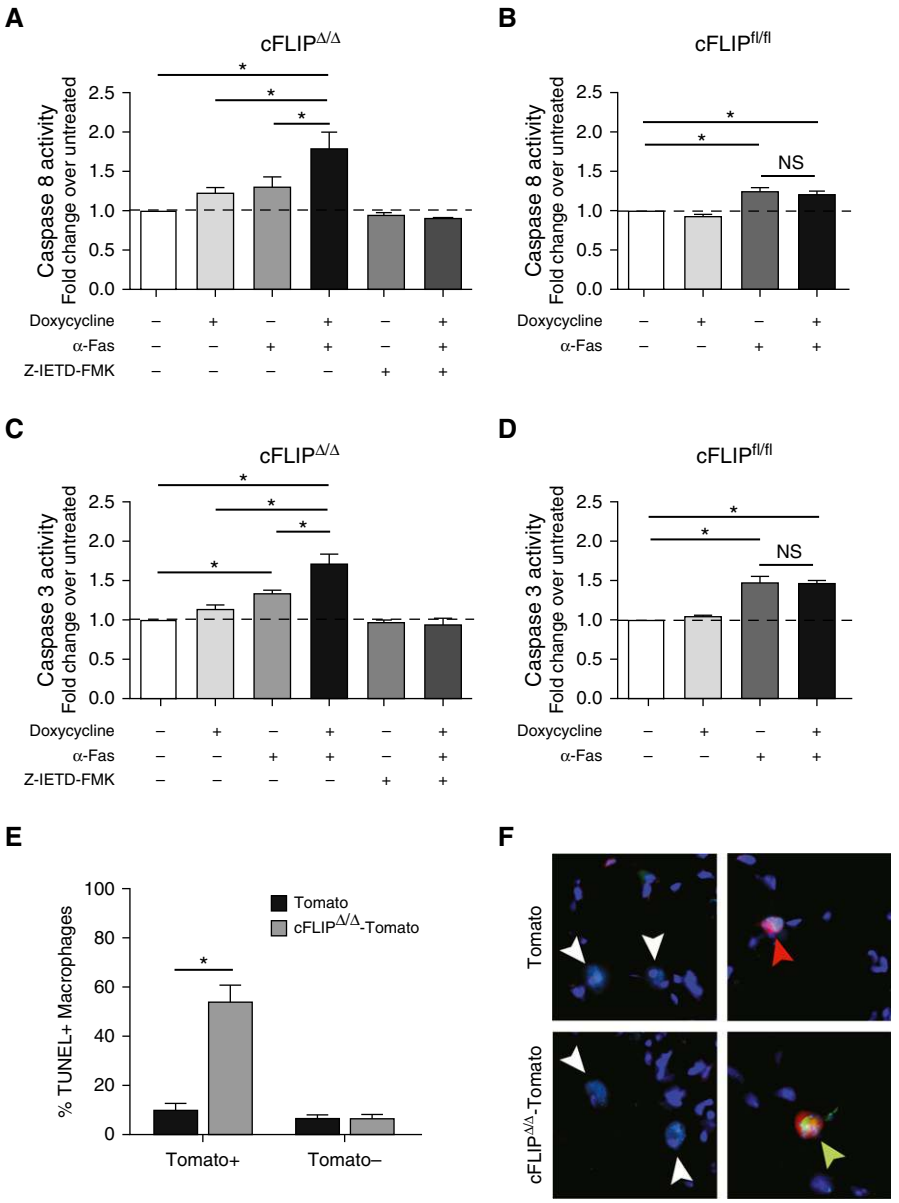

Figure 2. Cellular FADD-like IL-1β–converting enzyme–inhibitory protein (cFLIP)$^{\Delta/\Delta}$ mice delete c-FLIP in CD11b^{hi} MΦ and sensitize CD11b^{hi} MΦ to caspase-8–dependent cell death. (*A–D*) Caspase activity was measured using Caspase-Glo luminescent assays. MΦ were collected by lavage 7 days after bleomycin and treated with doxycycline (20 ng/ml) *in vitro* for 36 hours to induce deletion of c-FLIP. Doxycycline was removed and cells were treated with α-Fas activating antibody (5 μg/ml) for a further 8 hours (caspase-8) or 12 hours (caspase-3). Some wells were treated with the selective caspase-8 inhibitor, Z-IETD-FMK, at 10 μM for 30 minutes before α-Fas. (*A* and *B*) Caspase-8 activity of CD11b^{hi} MΦ from cFLIP$^{\Delta/\Delta}$ (*A*) or cFLIP$^{fl/fl}$ mice (*B*) after doxycycline treatment and/or stimulation with activating α-Fas antibody. (*C* and *D*) Caspase-3 activity of CD11b^{hi} MΦ from cFLIP$^{\Delta/\Delta}$ mice (*C*) or cFLIP$^{fl/fl}$ mice (*D*) after doxycycline treatment and stimulation with activating α-Fas antibody. (*E* and *F*) Control Tomato-reporter mice and cFLIP$^{\Delta/\Delta}$-Tomato mice were treated with bleomycin and then started on doxycycline at Day 7. At Day 10, lungs were collected, inflated, and frozen with optimal cutting temperature compound for histology. Double-stranded DNA breaks were labeled with terminal deoxynucleotidyl transferase dUTP nick end labeling (TUNEL; green), and tissue sections were costained with CD68 (teal) and DAPI (blue), along with endogenous Tomato reporter (red). Tomato^{+} and Tomato^{-} MΦ were counted and assessed for TUNEL positivity. Representative images are shown, with white arrowheads pointing to Tomato^{-} viable MΦ, the red arrowhead pointing to a Tomato^{+} viable MΦ, and the green arrowhead pointing to a TUNEL^{+} Tomato^{+} apoptotic MΦ. Data from $n = 4$–7 mice from three separate experiments shown as mean (±SEM). *$P < 0.05$. NS = not significant.

adherence and increased floating cells, also consistent with cell death (data not shown). Taken as a whole, these experiments demonstrate that c-FLIP deletion in lung MΦ amplifies caspase-8 activation in response to death receptor ligation, leading to downstream caspase-3 activation and cell death.

To confirm that loss of c-FLIP induced CD11b^{hi} MΦ cell death *in vivo*, we crossed cFLIP$^{\Delta/\Delta}$ to Rosa-stop$^{fl/fl}$-Tomato reporter mice (cFLIP$^{\Delta/\Delta}$-Tomato), such that administration of doxycycline simultaneously deletes c-FLIP in CD11b^{hi} MΦ and marks these MΦ with Tomato. Control animals were CD68rtTA × tetOn-cre × Rosa-stop$^{fl/fl}$-Tomato reporter mice (control-Tomato) that marked CD11b^{hi} MΦ with Tomato, but did not delete c-FLIP. cFLIP$^{\Delta/\Delta}$-Tomato and control-Tomato mice were treated with bleomycin; 7 days later, mice were started on doxycycline to delete c-FLIP. Lung sections were costained for CD68 to mark MΦ and terminal deoxynucleotidyl transferase dUTP nick end labeling (TUNEL) to mark dead cells (Figures 2E and 2F). In cFLIP$^{\Delta/\Delta}$-Tomato mice, TUNEL^{+} MΦ were increased in Tomato^{+} (i.e., c-FLIP deficient) but not Tomato^{-} (i.e., c-FLIP sufficient) MΦ. In contrast, in Tomato-reporter mice, low numbers of TUNEL^{+} cells were observed in both Tomato^{+} and Tomato^{-} MΦ. These data show that conditional deletion of c-FLIP *in vivo* results in MΦ death.

Deletion of c-FLIP from CD11b^{hi} MΦ Prevents Their Accumulation after Bleomycin

To assess the effect of c-FLIP deletion *in vivo*, we treated cFLIP$^{\Delta/\Delta}$ and littermate control mice (cFLIP$^{fl/fl}$) with bleomycin; 1 day later, mice were started on doxycycline. Delaying doxycycline treatment allowed us to avoid potential confounding effects of c-FLIP deletion on initial inflammation and injury. Previous hCD68rtTA reporter studies showed that maximum transgene expression takes at least 4 days, although expression began within 24 hours (16). The total number of lung MΦ in BAL and lung digest was enumerated on Days 0, 4, 7, and 14 (Figures 3A and 3B). Until Day 7, total MΦ numbers were similar between cFLIP$^{\Delta/\Delta}$ and cFLIP$^{fl/fl}$ mice. However, by Day 14, total numbers of MΦ were significantly lower in cFLIP$^{\Delta/\Delta}$ mice. This decrease in MΦ numbers was not due to a change in Siglec-F^{hi} MΦ, but rather to a loss of CD11b^{hi} MΦ in both the BAL and lung digest (Figures 3C–3F). Importantly, early inflammation was similar between c-FLIP$^{\Delta/\Delta}$ and cFLIP$^{fl/fl}$ mice; neutrophil, eosinophil, and monocyte numbers were equivalent (Figures E3A–E3D). Dendritic cells, which are targeted by hCD68rtTA (16), also had similar numbers between

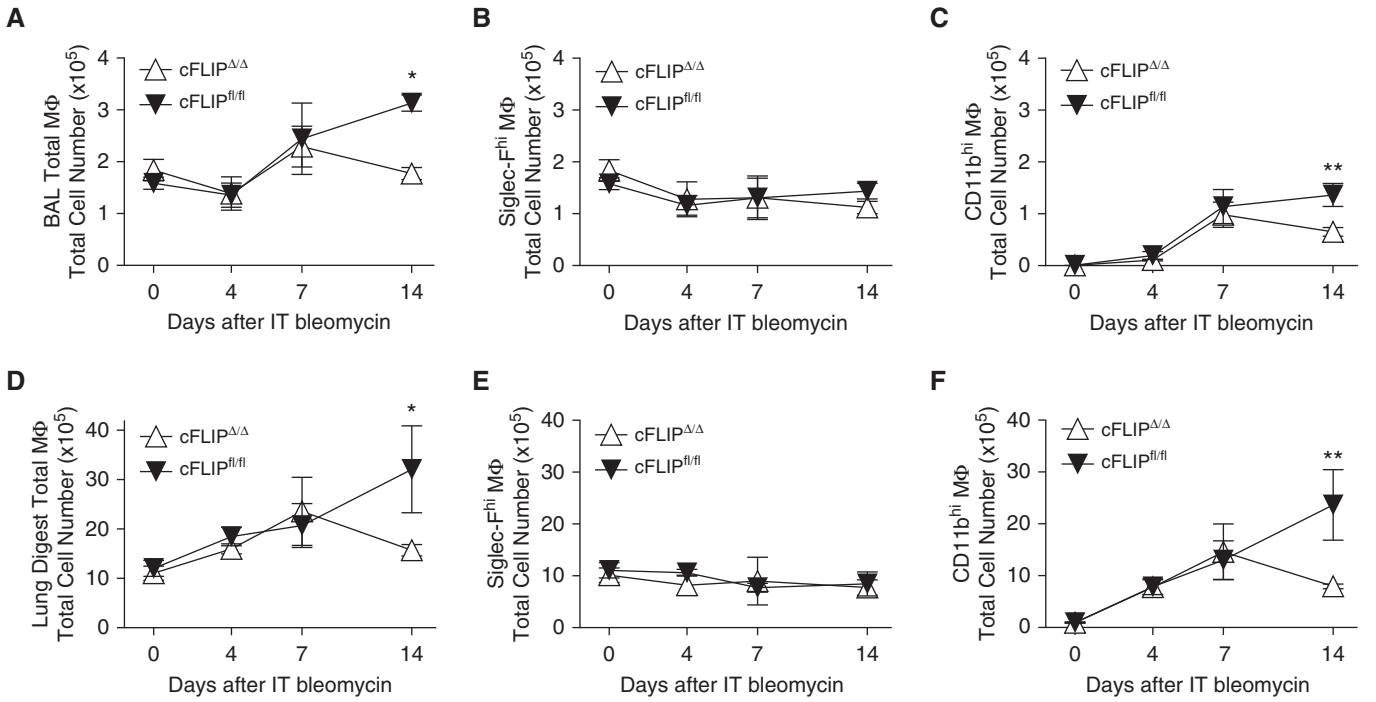

Figure 3. CD11b^{hi} MΦ, but not Siglec-F^{hi} MΦ, numbers are decreased in cFLIP$^{\Delta/\Delta}$ mice after bleomycin. Flow cytometry was used to assess total MΦ numbers 0, 4, 7, and 14 days after bleomycin in lavage and lung digests. cFLIP$^{\Delta/\Delta}$ and cFLIP$^{fl/fl}$ mice were started on doxycycline 1 day after bleomycin. (*A–C*) Total MΦ, Siglec-F^{hi} MΦ, and CD11b^{hi} MΦ numbers in BAL. (*D–F*) Total MΦ, SiglecF^{+} MΦ, and CD11b^{hi} MΦ numbers in lung digests. (*G*) Bleomycin-treated mice were given IT α-CD45 to label alveolar cells (IT CD45). BAL was performed 3 minutes later to sample alveolar cells and remove unbound antibody. Lung digestion was performed immediately after lavage. BAL and lung digest was processed for flow cytometry; Siglec-F^{hi} MΦ and CD11b^{hi} MΦ were separated as described in Figure 1A. IT CD45 staining is shown in BAL and lung digest. BAL staining acts as a positive control; lung digest from mice not given IT CD45 help set the negative gate. (*H*) CD11b^{hi} MΦ can be separated into high-and low-SSC populations using SSC versus CD11c. (*I*) Low-SSC CD11b^{hi} MΦ correlate with IT^{-} tissue MΦ, whereas high-SSC CD11b^{hi} MΦ correlate with IT^{+} alveolar MΦ. (*J*) Representative dot plots showing high- and low-SSC subpopulations in cFLIP$^{fl/fl}$ and cFLIP$^{\Delta/\Delta}$ mice 14 days after bleomycin. (*K*) Total numbers of high- and low-SSC CD11b^{hi} MΦ 14 days after bleomycin corresponding to alveolar and tissue CD11b^{hi} MΦ, respectively. Data from $n = 3$–5 mice/group shown as mean (±SEM). $^{*}P < 0.05$, $^{**}P < 0.01$.

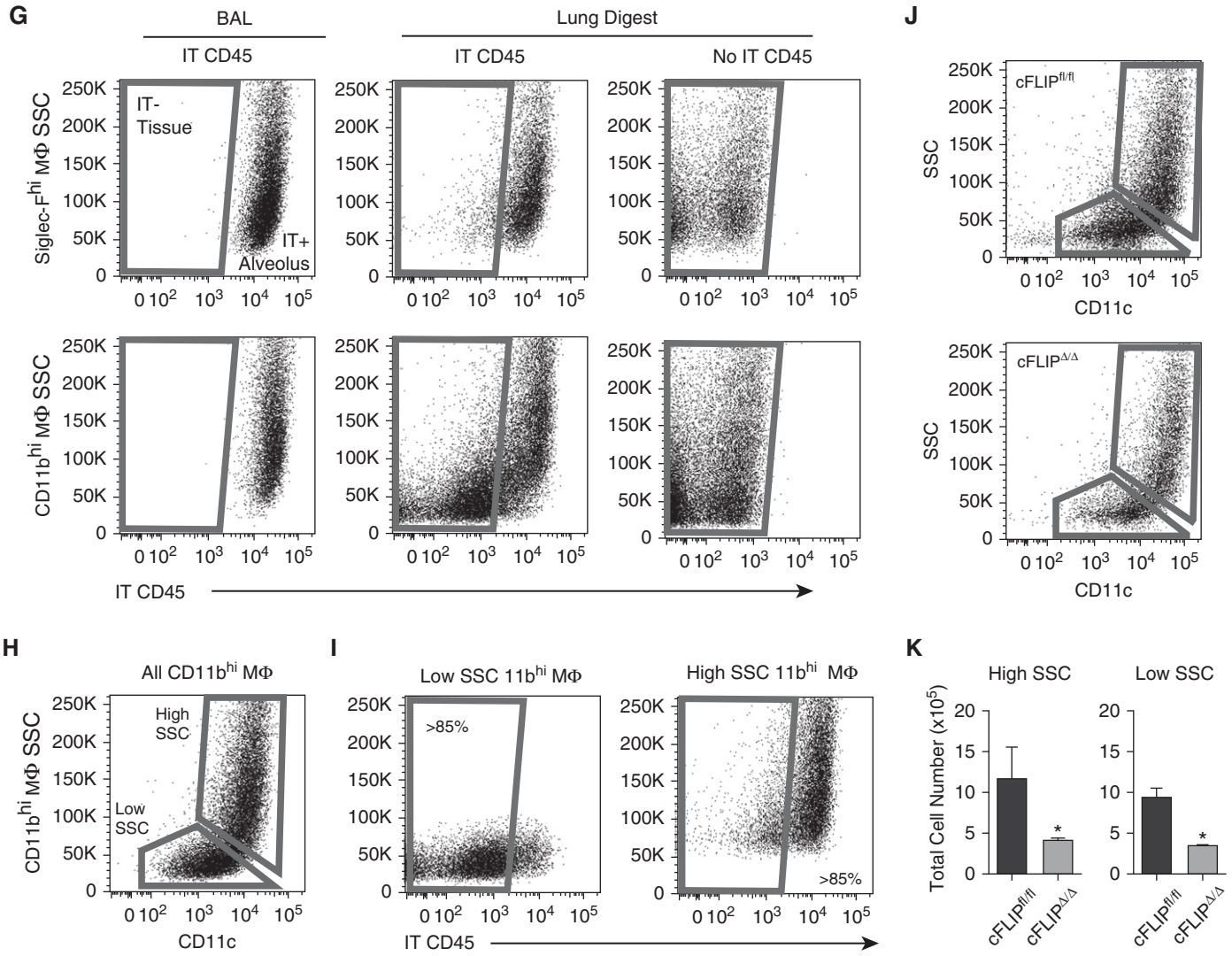

Figure 3. (Continued).

groups (Figures E3E–E3G). Furthermore, we have previously shown that no CD45-negative cells activate hCD68rtTA (16), but we verified that fibroblasts were not targeted in our system by staining lung sections from bleomycin-treated reporter mice with α-smooth muscle actin (Figure E4).

Because hCD68rtTA targets CD11b^{hi} MΦ in the airspaces and tissue during inflammation (16), we separated CD11b^{hi} MΦ by compartment to examine the effect of c-FLIP deletion. A fluorescently conjugated α-CD45 antibody was given intratracheally to bleomycin-treated mice immediately after being killed to selectively label MΦ in the airspaces (but not the tissues) (32). BAL was performed 5 minutes later, followed by lung digestion. As expected, both Siglec-F^{hi} MΦ and CD11b^{hi} MΦ from BAL stained brightly with intratracheal α-CD45 (Figure 3G). Siglec-F^{hi} MΦ present in lung digests also stained brightly with intratracheal α-CD45, confirming that Siglec-F^{hi} MΦ existed exclusively in the alveolus. These data also demonstrate that lavage is inefficient in removing leukocytes from the alveolus, as previously shown (33). Notably, when CD11b^{hi} MΦ from lung digests were examined for α-CD45 labeling, there were two populations. The first stained brightly with α-CD45, indicating that these cells were from the alveolar compartment and represented *recruited* CD11b^{hi} alveolar MΦ. The second population was α-CD45 dim, indicating that these CD11b^{hi} cells resided in the tissues and were IMs. Results were not compromised by any bleomycin- or BAL-induced damage of the tissue; intravenous α-CD45 given before death was not found in BAL, demonstrating that the lung tissue is intact (Figure E3H).

Careful examination of the α-CD45 dim (i.e., interstitial) and bright (i.e., alveolar) CD11b^{hi} MΦ populations revealed that their side scatter (SSC) profiles were different (Figure 3G), as was expression of CD11c (data not shown). We therefore hypothesized that SSC and CD11c might serve as markers of tissue localization. Indeed, separating CD11b^{hi} MΦ from lung digest using SSC versus CD11c isolated two populations (Figure 3H) that correlated highly with alveolar and tissue MΦ (Figure 3I). Application of this technique to lung

digests from cFLIP$^{\Delta/\Delta}$ versus cFLIP$^{fl/fl}$ mice confirmed that deletion of c-FLIP resulted in decreased numbers of CD11b^{hi} MΦ in both the interstitium and airspaces (Figures 3J and 3K). Taken as a whole, these results demonstrate that c-FLIP is required for maintenance of CD11b^{hi} MΦ in both the alveolus and lung tissue, and that deletion of c-FLIP reduces CD11b^{hi} MΦ numbers without impacting levels of other myeloid cell populations, including Siglec-F^{hi} resident alveolar MΦ.

Deletion of c-FLIP from CD11b^{hi} MΦ and Loss of CD11b^{hi} MΦ Protected Mice from the Development of Lung Fibrosis

Because inducible deletion of c-FLIP in CD11b^{hi} MΦ significantly reduces their numbers in the lung, we used this system to test the hypothesis that elimination of CD11b^{hi} MΦ would attenuate the development of fibrosis. As a first step, we treated cFLIP$^{\Delta/\Delta}$ and cFLIP$^{fl/fl}$ mice with bleomycin and began administration of doxycycline 1 day later. To provide a reference for noninjured lungs groups of cFLIP$^{\Delta/\Delta}$ and cFLIP$^{fl/fl}$, animals were given doxycycline without bleomycin. Fibrosis was assessed 14 days later using lung physiology, histology, and hydroxyproline measurements. As shown in Figure 4A, bleomycin-treated cFLIP$^{fl/fl}$ mice had a marked decrease in static lung compliance compared with healthy controls. Deletion of c-FLIP in CD11b^{hi} MΦ reversed this defect; static compliance in bleomycin-treated cFLIP$^{\Delta/\Delta}$ mice was similar to that in healthy controls. Similarly, lungs from bleomycin-treated cFLIP$^{fl/fl}$ mice demonstrated a marked increase in hydroxyproline content, whereas cFLIP$^{\Delta/\Delta}$ mice were protected (Figure 4B). Trichrome staining of cFLIP$^{\Delta/\Delta}$ and cFLIP$^{fl/fl}$ lungs showed patchy lung injury, typical of bleomycin. Larger areas of damage with inflammatory infiltrates and greater collagen deposition were observed in cFLIP$^{fl/fl}$ mice compared with cFLIP$^{\Delta/\Delta}$ mice (Figures 4C and 4D). Taken together, these studies suggest that early deletion of c-FLIP from CD11b^{hi} MΦ induces loss of CD11b^{hi} MΦ and attenuates fibrogenesis.

As shown in Figure 1, CD11b^{hi} MΦ numbers in wild-type mice were increased 7 days after bleomycin; however, fibrosis in this system does not peak until Day 14 (4). Ergo, we hypothesized that the CD11b^{hi}

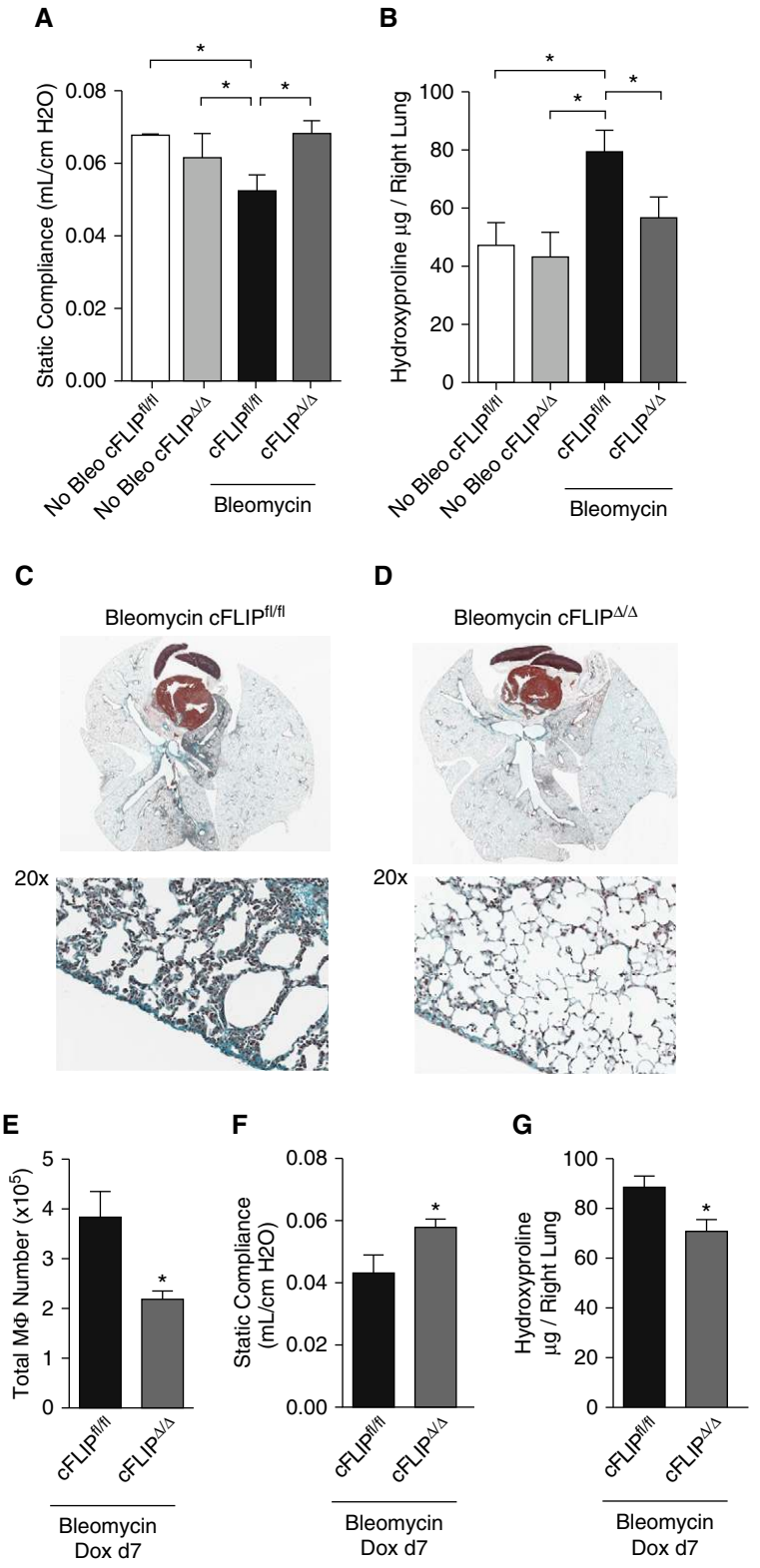

Figure 4. Deletion of c-FLIP from CD11b^{hi} MΦ protects against the development of fibrosis. cFLIP$^{fl/fl}$ and cFLIP$^{\Delta/\Delta}$ mice were treated with bleomycin and started on doxycycline 1 day later; fibrosis was assessed at Day 14. Doxycycline-only controls comprised of both cFLIP$^{fl/fl}$ and cFLIP$^{\Delta/\Delta}$ mice were given doxycycline for a matched 13 days before death. (*A*) Static compliance measured by flexiVent. (*B*) Hydroxyproline levels in the right lung. (*C* and *D*) Trichrome stain on paraffin-embedded lung

MΦ present 7–14 days after bleomycin were particularly important for the development of fibrosis. To test this, we treated mice with bleomycin, but waited 7 days before administering doxycycline. At Day 14, MΦ numbers were decreased in cFLIP$^{\Delta/\Delta}$ mice (Figure 4E), which were again protected from the development of fibrosis, as demonstrated by improved lung compliance and decreased hydroxyproline content (Figures 4F and 4G). These findings suggest that CD11b^{hi} MΦ present in the lungs 7–14 days after bleomycin promote the development of fibrosis.

CD11b^{hi} MΦ Are Distinct from Siglec-F^{hi} MΦ with High Expression of Profibrotic Chemokines after Bleomycin Injury

To investigate how CD11b^{hi} MΦ might promote lung fibrosis, we performed RNA-seq analysis of CD11b^{hi} MΦ and SiglecF^{hi} MΦ from wild-type mice after bleomycin (GEO accession no. GSE94699). Based on our data showing a profibrotic role for CD11b^{hi} MΦ present 7–14 days after bleomycin, we chose to assess MΦ populations within this window, and isolated naive SiglecF^{hi} MΦ and CD11b^{hi} MΦ and SiglecF^{hi} MΦ on Day 8. Our novel RNA-seq was merged with published RNA-seq of resident IMs and SiglecF^{hi} MΦ from naive mice (GEO accession no. GSE94135) (31). Pearson correlation showed that CD11b^{hi} MΦ sorted 8 days after bleomycin were a distinct population from Siglec-F^{hi} MΦ and naive IMs (Figure 5A). In contrast, Siglec-F^{hi} MΦ were remarkably similar, whether collected from naive or bleomycin-treated lungs. The most up- and downregulated genes are shown in the data supplement (Figure E5). To validate our sort strategy, we confirmed that all MΦ showed high expression of commonly accepted MΦ markers and low expression of genes associated with lymphocytes, dendritic cells, neutrophils, and eosinophils (Figure 5B).

Many researchers frame MΦ in terms of having an "M1" or "M2" polarization, where M2 is associated with prorepair or profibrotic MΦ. However, we and others have questioned the ability of a binary system to describe the complexities of MΦ polarization, particularly *in vivo* (34–36). RNA-seq showed that CD11b^{hi} and Siglec-F^{hi} MΦ from bleomycin-treated mice expressed markers of both M1 and M2 polarization (Figure E6). Expression of these markers by the two MΦ subtypes was largely similar. In aggregate, the transcriptomal profiles of CD11b^{hi} and Siglec-F^{hi} MΦ highlight the problem of ascribing a facile polarization state to MΦ populations *in vivo*. With this in mind, we sought to explore pathways that relate directly to fibrosis.

Closer inspection of the RNA-seq data showed that CD11b^{hi} MΦ had higher expression of epithelial and fibroblast proliferative factors (37), including hepatocyte growth factor, as well as higher expression of matrix-remodeling proteins (Figure E7A). More strikingly, CD11b^{hi} MΦ showed elevated expression of numerous chemokines compared with Siglec-F^{hi} MΦ (Figure 6A), many with established profibrotic functions, including *ccl2*, *ccl12*, and *ccl24* (38).

Human BAL MΦ from Patients with IPF Show High Expression of Profibrotic Chemokines

To determine if human and murine MΦ from fibrotic lungs share common features that drive fibrosis, we used publically available gene-array data from the GEO to assess the overlap of our murine CD11b^{hi} MΦ profibrotic MΦ with the signatures of BAL MΦ from patients with IPF (29) (GEO accession no. GSE49072). Most structural cell mitogens and matrix-remodeling proteins, although upregulated in murine CD11b^{hi} MΦ, were not upregulated in BAL MΦ from patients with IPF (Figure E7B). However, profibrotic chemokines were strongly upregulated in BAL MΦ from patients with IPF (Figure 6B); this overlapped with a group of murine homologs expressed by CD11b^{hi} MΦ. Interestingly, this overlap comprised chemokines that recruit fibrocytes to the lung and promote fibroblast survival, including *ccl2* and *ccl24* (39–41). Although the human alveolar MΦ were obtained from patients with established fibrosis (rather than the initiation phase), and were not divided into resident versus recruited subsets, these data suggest that one common mechanism by which murine and human MΦ contribute to the development of fibrosis may be elevated production of profibrotic chemokines that stimulate recruitment and survival of fibrocytes and fibroblasts.

In summary, we show that murine CD11b^{hi} MΦ promote the development of lung fibrosis after bleomycin. Using hCD68rtTA, we were able to delete c-FLIP in CD11b^{hi} MΦ and induce CD11b^{hi} MΦ death after bleomycin. Loss of CD11b^{hi} MΦ was sufficient to prevent the development of fibrosis. RNA-seq suggests that this profibrotic function may be mediated through production of profibrotic factors, including chemokines specifically expressed by CD11b^{hi} MΦ.

Discussion

MΦ in the lungs can be divided into multiple subsets. Identifying their relative contributions to the development of fibrosis has become an important area of research. In this study, we provide a clear flow cytometry strategy to separate resident alveolar MΦ (Siglec-F^{hi}) from other MΦ present during fibrosis (CD11b^{hi}), the majority of which are recruited MΦ that arise from immigrating monocytes. Using the novel hCD68rtTA system (16), we were able to discretely target CD11b^{hi} MΦ without affecting Siglec-F^{hi} MΦ, and demonstrate the specific contribution of CD11b^{hi} MΦ to the development of bleomycin-induced fibrosis.

Using established MΦ markers, CD64 and Mertk (30, 31), we could clearly select MΦ within the BAL or lung digest. Recruited CD11b^{hi} MΦ in the alveolus adopt a resident-like phenotype over time, including down-regulation of CD11b, which can make their distinction difficult during the late phases of inflammation (42). However, we have identified high Siglec-F as a persistent marker of resident alveolar MΦ (7), and were able to leverage this

Figure 4. (Continued). sections from mice started on doxycycline 1 day after bleomycin and isolated at Day 14. Collagen stains blue–green. Zoom image of pleural surface highlights collagen deposition. (*E–G*) cFLIP$^{fl/fl}$ and cFLIP$^{\Delta/\Delta}$ mice were treated with bleomycin and started on doxycycline 7 days later. Fibrosis was assessed at Day 14. (*E*) MΦ numbers from lung digest of the left lung. (*F*) Static compliance measured by flexiVent. (*G*) Hydroxyproline content in the right lung. Data from $n = 6$–11 mice/group shown as mean (±SEM). *$P < 0.05$. Bleo = bleomycin; Dox = doxycycline.

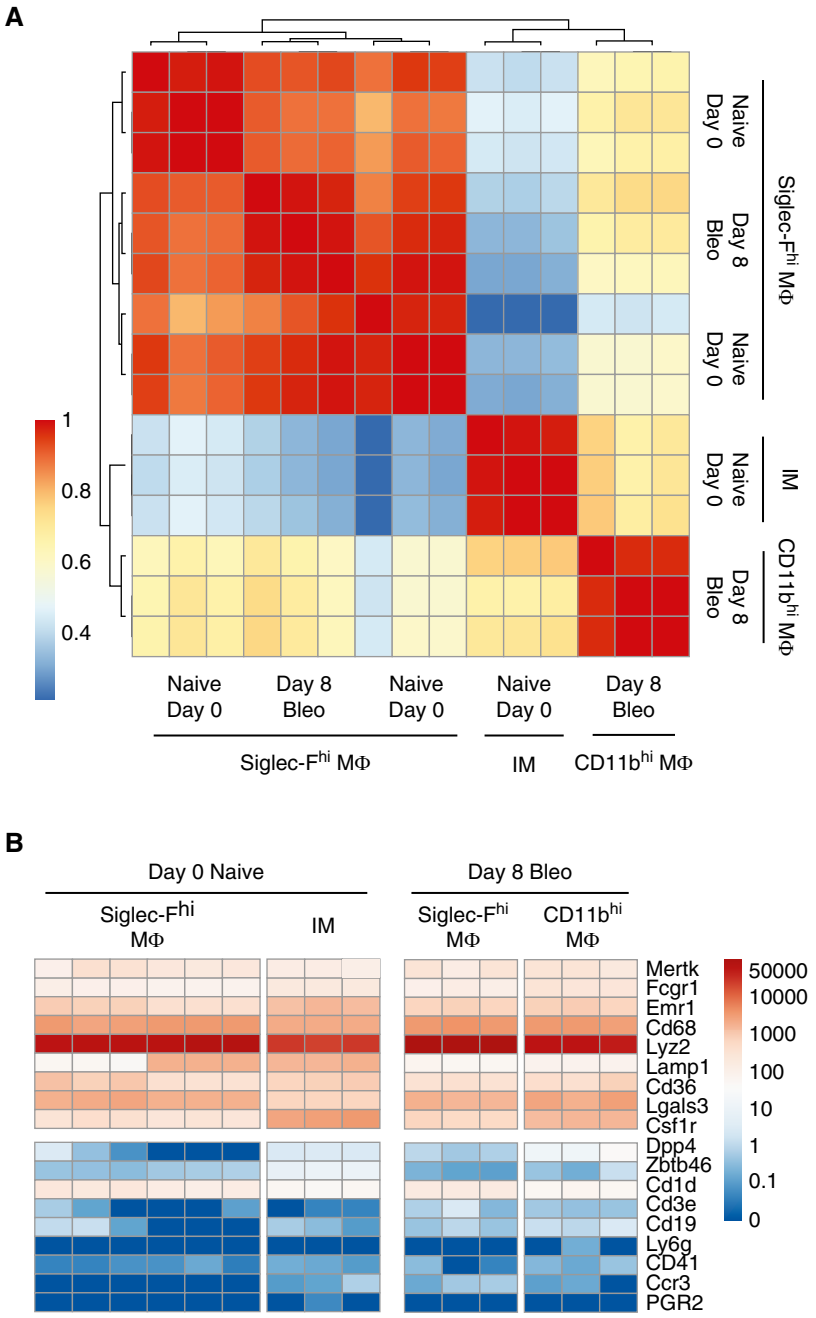

Figure 5. Global analysis of CD11b^{hi} MΦ and Siglec-F^{hi} MΦ transcriptomes shows that the two MΦ populations are distinct. Resident Siglec-F^{hi} alveolar MΦ or resident interstitial MΦ (IMs) from naive lungs (naive Day 0), and Siglec-F^{hi} and CD11b^{hi} MΦ from bleomycin-treated lungs after 8 days (Day 8 bleo) were sorted for RNA-seq analysis. (*A*) Individual replicates of Siglec-F^{hi} MΦ of IMs from naive lungs and Siglec-F^{hi} MΦ and CD11b^{hi} MΦ from bleomycin-treated lungs compared using pairwise Pearson correlation. (*B*) Heat map showing gene expression in transcripts per million (TPM) on a log scale of MΦ-lineage–associated genes and non–MΦ-lineage–associated genes.

observation to separate resident alveolar MΦ from other lung MΦ at all time points examined.

Importantly, we recently described a new inducible transgenic system, hCD68rtTA, capable of targeting CD11b^{hi} IMs and recruited MΦ in the lung without affecting resident Siglec-F^{hi} MΦ. Traditional cre drivers, such as lysozyme M and colony stimulating factor 1 receptor, do not distinguish between MΦ subsets, and have considerable overlap with other myeloid cells. hCD68rtTA is the first transgenic system to discretely target CD11b^{hi} MΦ in the lung, presenting a unique opportunity to study their function. Using this system, we were able to manipulate the survival of CD11b^{hi} MΦ by deleting the antiapoptotic protein, c-FLIP, and thus study their function during fibrogenesis.

Previous approaches to target CD11b^{hi} MΦ have relied on blocking their monocyte precursors (3, 11, 43). These techniques unavoidably impact all monocyte-derived cells, including dendritic cells and fibrocytes (41), as well as Ly6C^{hi} inflammatory monocytes themselves, altering the early inflammatory response to bleomycin. With these confounding off-target effects, it has been difficult to isolate the importance of CD11b^{hi} MΦ. Our hCD68rtTA system improves on this in two ways: first, by directly targeting only 60% of monocytes compared with nearly 90% of CD11b^{hi} MΦ (16); second, c-FLIP expression is very low in monocytes, but strongly upregulated upon differentiation to MΦ (24). Accordingly, we found no evidence that monocytes were directly altered by loss of c-FLIP: early recruitment of CD11b^{hi} MΦ was matched between cFLIP$^{\Delta/\Delta}$ and cFLIP$^{fl/fl}$ mice, and monocyte recruitment to the alveolus was matched at all time points examined. Also importantly, fibroblasts are not targeted in our system; no α-smooth muscle actin^{+} or CD45^{-} cells had reporter expression. Moreover, we found no change in the numbers of any leukocyte population besides CD11b^{hi} MΦ in cFLIP$^{\Delta/\Delta}$ mice. Therefore, cFLIP$^{\Delta/\Delta}$ mice discretely induce the death of CD11b^{hi} MΦ.

In addition to superior targeting, deletion of c-FLIP was only induced upon administration of doxycycline. Taking advantage of this inducible system, we delayed doxycycline administration to exactly match initial injury between cFLIP$^{\Delta/\Delta}$ and cFLIP$^{fl/fl}$ mice, and define the window of CD11b^{hi} MΦ action. For our initial studies, we began doxycycline 1 day after bleomycin; this substantially blocked the development of fibrosis. Waiting to administer doxycycline until 7 days after bleomycin afforded the same level of protection. Therefore, CD11b^{hi} MΦ present in the lungs 7–14 days after bleomycin promote the development of fibrosis, whereas CD11b^{hi} MΦ present between Days 1 and 7 do not. This model

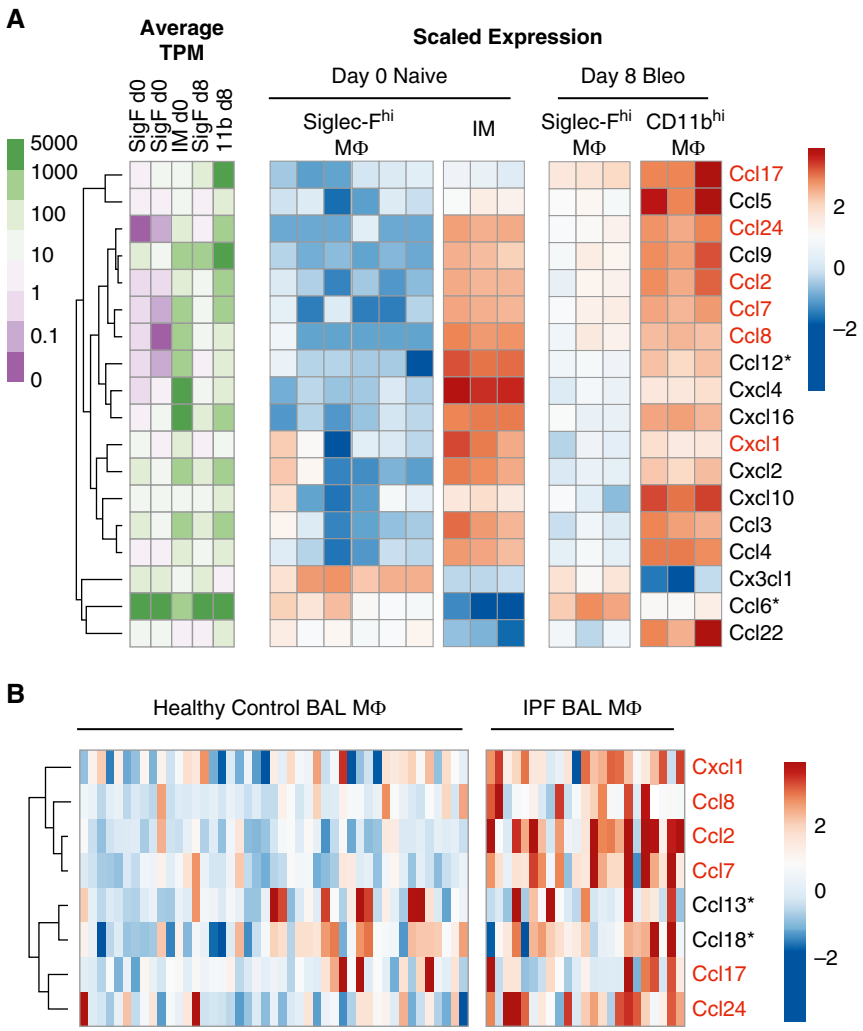

Figure 6. CD11b^{hi} MΦ express a profibrotic signature, including high expression of multiple profibrotic chemokines, that is validated in human MΦ from patients with idiopathic pulmonary fibrosis (IPF). (*A*) Heat maps showing expression of genes encoding chemokines. Unsupervised clustering was used to highlight associations between expression of these genes and MΦ subtypes. Raw expression is displayed on a log scale as average TPM per group (green–purple color scale) and scaled expression shows relative expression of each gene as the change from row mean scaled to a standard deviation of 1 (red–blue color scale). (*B*) Chemokines with significantly different expression in BAL MΦ from patients with IPF compared with normal volunteers were identified from publically available data in the Gene Expression Omnibus (accession no. GSE49072). Unsupervised clustering was used to highlight associations between expression of these genes and disease state. Scaled expression shows relative expression of each gene as the change from row mean scaled to a standard deviation of 1. Chemokines upregulated in both human IPF MΦ and murine CD11b^{hi} MΦ compared with control human MΦ or murine SiglecF^{hi} MΦ after bleomycin are highlighted in *red*. *Gene with no direct murine/human homolog.

may be adapted further, for example, by delaying doxycycline until after fibrosis has developed to test whether inducing CD11b^{hi} MΦ death will accelerate the resolution of established fibrosis.

RNA-seq suggested multiple means by which CD11b^{hi} MΦ might exert a profibrotic function. We observed that CD11b^{hi} MΦ are the predominant MΦ source of profibrotic chemokines, matrix remodeling proteins, and growth factors for epithelial cells and fibroblasts. Interestingly, we found that elevated expression of fibrogenic chemokines was echoed in human lavaged MΦ from patients with IPF. In particular, *ccl2* and *ccl24* were strongly upregulated in murine CD11b^{hi} MΦ isolated from bleomycin-treated mice and in human MΦ from patients with IPF. In humans and mice, these chemokines can directly recruit fibrocytes to the lung. CCL24 also promotes the survival of fibroblasts, whereas CCL2 stimulates their proliferation and production of collagen (39, 40, 44, 45). CCL2 and CCL24 correlate with progression and severity of human IPF (46, 47). We speculate that production of CCL2 and CCL24 by CD11b^{hi} MΦ is one mechanism by which CD11b^{hi} MΦ promote the development of fibrosis, which can be clarified in future studies. In addition, it is notable that the addition of exogenous apoptotic cells accelerates the resolution of fibrosis in mice (48). Accordingly, it is possible that inducing the death of CD11b^{hi} MΦ in cFLIP$^{\Delta/\Delta}$ mice both removed a profibrotic signal and provided a resolving one.

Targeting profibrotic CD11b^{hi} MΦ may be valuable in the treatment of fibrosis. We were able to induce the death of CD11b^{hi} MΦ by deleting c-FLIP, an apoptosis inhibitor downstream of death receptor ligation. This pathway is ripe for pharmacologic intervention. c-FLIP inhibitors, currently in development as antitumor drugs, may be used to block this key antiapoptotic regulator and sensitize profibrotic MΦ to death. Alternately, or even simultaneously, immunotherapies could focus on the exogenous addition of death ligands like FasL or TNF-α, increasing proapoptotic signals. Supporting this direction, administration of TNF-α to bleomycin-treated mice was shown to accelerate the resolution of fibrosis (4). Profibrotic mediators produced by CD11b^{hi} MΦ may also be fruitful targets. We speculate that CCL2 and CCL24 are key profibrotic chemokines. Although initial testing of α-CCL2 immunotherapy was halted due to complications (49), α-CCL24 immunotherapy is in development, and may be useful in the treatment of IPF.

Because much of the MΦ literature in lung fibrosis has focused on MΦ polarization, it is important to note that RNA-seq did not identify a clear M1 or M2 polarization in Siglec-F^{hi} or CD11b^{hi} MΦ. Although individual genes can be selected to argue for a specific polarization (i.e., *Arg1*), looking at the body of markers clearly demonstrates that both M1 and M2 pathways are

activated in lung MΦ. Although this could reflect the presence of discrete M1 and M2 polarized subpopulations within MΦ subtypes (testable by single-cell analysis), our data best support the view that a binary system is not capable of categorizing the complex MΦ present in disease states (34, 36).

In contrast, separating subsets and studying functionality of MΦ provides important insight into disease pathology. We clearly show that CD11b^{hi} MΦ drive fibrogenesis, whereas resident Siglec-F^{hi} alveolar MΦ neither increase in number after bleomycin nor express high levels of profibrotic mediators. Nonetheless, our study is only a first step toward clarifying the complex MΦ subsets present in the lung during fibrosis. In the future, we anticipate that it will be possible to further divide CD11b^{hi} MΦ into resident IMs and recruited alveolar and tissue MΦ. It is intriguing that naive IMs express many chemokines and matrix-remodeling factors that can be considered profibrotic. Because cell origin and tissue environment shape MΦ function, phenotype, and transcriptome (7, 50, 51), whether alveolar and tissue CD11b^{hi} MΦ are equally profibrotic is an interesting question for further study. Because hCD68rtTA targets both alveolar and tissue CD11b^{hi} MΦ, our study was unable to address this question.

In summary, we have clearly identified CD11b^{hi} MΦ as key participants in the development of fibrosis. Targeted induction of CD11b^{hi} MΦ death prevents lung fibrosis. RNA-seq shows that CD11b^{hi} MΦ are the MΦ source of profibrotic factors, particularly chemokines. Up-regulation of the same profibrotic chemokines is observed in human alveolar MΦ from patients with IPF. CD11b^{hi} MΦ promote lung fibrogenesis, likely through the production of factors that support recruitment, growth, and differentiation of fibrocytes, fibroblasts, and myofibroblasts. ■

Author disclosures are available with the text of this article at www.atsjournals.org.

References

1. Schwartz DA, Helmers RA, Dayton CS, Merchant RK, Hunninghake GW. Determinants of bronchoalveolar lavage cellularity in idiopathic pulmonary fibrosis. *J Appl Physiol (1985)* 1991;71: 1688–1693.
2. Byrne AJ, Maher TM, Lloyd CM. Pulmonary macrophages: a new therapeutic pathway in fibrosing lung disease? *Trends Mol Med* 2016; 22:303–316.
3. Osterholzer JJ, Olszewski MA, Murdock BJ, Chen GH, Erb-Downward JR, Subbotina N, *et al*. Implicating exudate macrophages and Ly-6C(high) monocytes in CCR2-dependent lung fibrosis following gene-targeted alveolar injury. *J Immunol* 2013;190:3447–3457.
4. Redente EF, Keith RC, Janssen W, Henson PM, Ortiz LA, Downey GP, *et al*. Tumor necrosis factor-α accelerates the resolution of established pulmonary fibrosis in mice by targeting profibrotic lung macrophages. *Am J Respir Cell Mol Biol* 2014;50:825–837.
5. Scott CL, Henri S, Guilliams M. Mononuclear phagocytes of the intestine, the skin, and the lung. *Immunol Rev* 2014;262:9–24.
6. Epelman S, Lavine KJ, Randolph GJ. Origin and functions of tissue macrophages. *Immunity* 2014;41:21–35.
7. Gibbings SL, Goyal R, Desch AN, Leach SM, Prabagar M, Atif SM, *et al*. Transcriptome analysis highlights the conserved difference between embryonic and postnatal-derived alveolar macrophages. *Blood* 2015; 126:1357–1366.
8. Hashimoto D, Chow A, Noizat C, Teo P, Beasley MB, Leboeuf M, *et al*. Tissue-resident macrophages self-maintain locally throughout adult life with minimal contribution from circulating monocytes. *Immunity* 2013;38: 792–804.
9. Guilliams M, De Kleer I, Henri S, Post S, Vanhoutte L, De Prijck S, *et al*. Alveolar macrophages develop from fetal monocytes that differentiate into long-lived cells in the first week of life via GM-CSF. *J Exp Med* 2013;210:1977–1992.
10. Janssen WJ, Barthel L, Muldrow A, Oberley-Deegan RE, Kearns MT, Jakubzick C, *et al*. Fas determines differential fates of resident and recruited macrophages during resolution of acute lung injury. *Am J Respir Crit Care Med* 2011;184:547–560.
11. Okuma T, Terasaki Y, Kaikita K, Kobayashi H, Kuziel WA, Kawasuji M, *et al*. C-C chemokine receptor 2 (CCR2) deficiency improves bleomycin-induced pulmonary fibrosis by attenuation of both macrophage infiltration and production of macrophage-derived matrix metalloproteinases. *J Pathol* 2004;204:594–604.
12. Tsou CL, Peters W, Si Y, Slaymaker S, Aslanian AM, Weisberg SP, *et al*. Critical roles for CCR2 and MCP-3 in monocyte mobilization from bone marrow and recruitment to inflammatory sites. *J Clin Invest* 2007;117:902–909.
13. Lech M, Anders HJ. Macrophages and fibrosis: how resident and infiltrating mononuclear phagocytes orchestrate all phases of tissue injury and repair. *Biochim Biophys Acta* 2013;1832:989–997.
14. Misharin AV, Morales-Nebreda L, Mutlu GM, Budinger GR, Perlman H. Flow cytometric analysis of macrophages and dendritic cell subsets in the mouse lung. *Am J Respir Cell Mol Biol* 2013;49:503–510.
15. Zaynagetdinov R, Sherrill TP, Kendall PL, Segal BH, Weller KP, Tighe RM, *et al*. Identification of myeloid cell subsets in murine lungs using flow cytometry. *Am J Respir Cell Mol Biol* 2013;49:180–189.
16. McCubbrey AL, Barthel L, Mould KJ, Mohning MP, Redente EF, Janssen WJ. Selective and inducible targeting of CD11b+ mononuclear phagocytes in the murine lung with hCD68-rtTA transgenic systems. *Am J Physiol Lung Cell Mol Physiol* 2016;311:L87–L100.
17. Larson-Casey JL, Deshane JS, Ryan AJ, Thannickal VJ, Carter AB. Macrophage Akt1 kinase–mediated mitophagy modulates apoptosis resistance and pulmonary fibrosis. *Immunity* 2016;44:582–596.
18. Lamkanfi M, Festjens N, Declercq W, Vanden Berghe T, Vandenabeele P. Caspases in cell survival, proliferation and differentiation. *Cell Death Differ* 2007;14:44–55.
19. Green DR, Oberst A, Dillon CP, Weinlich R, Salvesen GS. RIPK-dependent necrosis and its regulation by caspases: a mystery in five acts. *Mol Cell* 2011;44:9–16.
20. Weinlich R, Dillon CP, Green DR. Ripped to death. *Trends Cell Biol* 2011;21:630–637.
21. Oztürk S, Schleich K, Lavrik IN. Cellular FLICE-like inhibitory proteins (c-FLIPs): fine-tuners of life and death decisions. *Exp Cell Res* 2012; 318:1324–1331.
22. Safa AR. c-FLIP, a master anti-apoptotic regulator. *Exp Oncol* 2012;34: 176–184.
23. Bagnoli M, Canevari S, Mezzanzanica D. Cellular FLICE-inhibitory protein (c-FLIP) signalling: a key regulator of receptor-mediated apoptosis in physiologic context and in cancer. *Int J Biochem Cell Biol* 2010;42:210–213.
24. Perlman H, Pagliari LJ, Georganas C, Mano T, Walsh K, Pope RM. FLICE-inhibitory protein expression during macrophage differentiation confers resistance to fas-mediated apoptosis. *J Exp Med* 1999;190:1679–1688.
25. Gordy C, Pua H, Sempowski GD, He YW. Regulation of steady-state neutrophil homeostasis by macrophages. *Blood* 2011;117:618–629.
26. Wu YJ, Wu YH, Mo ST, Hsiao HW, He YW, Lai MZ. Cellular FLIP inhibits myeloid cell activation by suppressing selective innate signaling. *J Immunol* 2015;195:2612–2623.
27. Zhang N, He YW. An essential role for c-FLIP in the efficient development of mature T lymphocytes. *J Exp Med* 2005;202:395–404.
28. Frankel SK, Moats-Staats BM, Cool CD, Wynes MW, Stiles AD, Riches DW. Human insulin-like growth factor-IA expression in transgenic mice promotes adenomatous hyperplasia but not pulmonary fibrosis. *Am J Physiol Lung Cell Mol Physiol* 2005;288:L805–L812.
29. Shi Y, Gochuico BR, Yu G, Tang X, Osorio JC, Fernandez IE, *et al*. Syndecan-2 exerts antifibrotic effects by promoting caveolin-1–mediated transforming growth factor-β receptor I internalization and

inhibiting transforming growth factor-β1 signaling. *Am J Respir Crit Care Med* 2013;188:831–841.
30. Gautier EL, Shay T, Miller J, Greter M, Jakubzick C, Ivanov S, *et al*.; Immunological Genome Consortium. Gene-expression profiles and transcriptional regulatory pathways that underlie the identity and diversity of mouse tissue macrophages. *Nat Immunol* 2012;13: 1118–1128.
31. Gibbings SL, Thomas SM, Atif SM, McCubbrey AL, Desch AN, Danhorn T, *et al*. Three unique interstitial macrophages in the murine lung at steady state. *Am J Respir Cell Mol Biol* 2017;57:66–76.
32. Patel BV, Tatham KC, Wilson MR, O'Dea KP, Takata M. *In vivo* compartmental analysis of leukocytes in mouse lungs. *Am J Physiol Lung Cell Mol Physiol* 2015;309:L639–L652.
33. Downey GP, Worthen GS, Henson PM, Hyde DM. Neutrophil sequestration and migration in localized pulmonary inflammation: capillary localization and migration across the interalveolar septum. *Am Rev Respir Dis* 1993;147:168–176.
34. Martinez FO, Gordon S. The M1 and M2 paradigm of macrophage activation: time for reassessment. *F1000Prime Rep* 2014;6:13.
35. Adhyatmika A, Putri KS, Beljaars L, Melgert BN. The elusive antifibrotic macrophage. *Front Med (Lausanne)* 2015;2:81.
36. Xue J, Schmidt SV, Sander J, Draffehn A, Krebs W, Quester I, *et al*. Transcriptome-based network analysis reveals a spectrum model of human macrophage activation. *Immunity* 2014;40:274–288.
37. Kendall RT, Feghali-Bostwick CA. Fibroblasts in fibrosis: novel roles and mediators. *Front Pharmacol* 2014;5:123.
38. Tomankova T, Kriegova E, Liu M. Chemokine receptors and their therapeutic opportunities in diseased lung: far beyond leukocyte trafficking. *Am J Physiol Lung Cell Mol Physiol* 2015;308:L603–L618.
39. Isgrò M, Bianchetti L, Marini MA, Bellini A, Schmidt M, Mattoli S. The C-C motif chemokine ligands CCL5, CCL11, and CCL24 induce the migration of circulating fibrocytes from patients with severe asthma. *Mucosal Immunol* 2013;6:718–727.
40. Kohan M, Puxeddu I, Reich R, Levi-Schaffer F, Berkman N. Eotaxin-2/CCL24 and eotaxin-3/CCL26 exert differential profibrogenic effects on human lung fibroblasts. *Ann Allergy Asthma Immunol* 2010;104:66–72.
41. Moore BB, Kolodsick JE, Thannickal VJ, Cooke K, Moore TA, Hogaboam C, *et al*. CCR2-mediated recruitment of fibrocytes to the alveolar space after fibrotic injury. *Am J Pathol* 2005;166:675–684.
42. Guth AM, Janssen WJ, Bosio CM, Crouch EC, Henson PM, Dow SW. Lung environment determines unique phenotype of alveolar macrophages. *Am J Physiol Lung Cell Mol Physiol* 2009;296: L936–L946.
43. Gibbons MA, MacKinnon AC, Ramachandran P, Dhaliwal K, Duffin R, Phythian-Adams AT, *et al*. Ly6C^{hi} monocytes direct alternatively activated profibrotic macrophage regulation of lung fibrosis. *Am J Respir Crit Care Med* 2011;184:569–581.
44. Murray LA, Argentieri RL, Farrell FX, Bracht M, Sheng H, Whitaker B, *et al*. Hyper-responsiveness of IPF/UIP fibroblasts: interplay between TGFbeta1, IL-13 and CCL2. *Int J Biochem Cell Biol* 2008;40: 2174–2182.
45. Ekert JE, Murray LA, Das AM, Sheng H, Giles-Komar J, Rycyzyn MA. Chemokine (C-C motif) ligand 2 mediates direct and indirect fibrotic responses in human and murine cultured fibrocytes. *Fibrogenesis Tissue Repair* 2011;4:23.
46. Baran CP, Opalek JM, McMaken S, Newland CA, O'Brien JM Jr, Hunter MG, *et al*. Important roles for macrophage colony-stimulating factor, CC chemokine ligand 2, and mononuclear phagocytes in the pathogenesis of pulmonary fibrosis. *Am J Respir Crit Care Med* 2007;176:78–89.
47. Foster MW, Morrison LD, Todd JL, Snyder LD, Thompson JW, Soderblom EJ, *et al*. Quantitative proteomics of bronchoalveolar lavage fluid in idiopathic pulmonary fibrosis. *J Proteome Res* 2015; 14:1238–1249.
48. Yoon YS, Kim SY, Kim MJ, Lim JH, Cho MS, Kang JL. PPARγ activation following apoptotic cell instillation promotes resolution of lung inflammation and fibrosis via regulation of efferocytosis and proresolving cytokines. *Mucosal Immunol* 2015;8: 1031–1046.
49. Raghu G, Martinez FJ, Brown KK, Costabel U, Cottin V, Wells AU, *et al*. CC-chemokine ligand 2 inhibition in idiopathic pulmonary fibrosis: a phase 2 trial of carlumab. *Eur Respir J* 2015;46:1740–1750.
50. Lavin Y, Winter D, Blecher-Gonen R, David E, Keren-Shaul H, Merad M, *et al*. Tissue-resident macrophage enhancer landscapes are shaped by the local microenvironment. *Cell* 2014;159:1312–1326.
51. Gundra UM, Girgis NM, Ruckerl D, Jenkins S, Ward LN, Kurtz ZD, *et al*. Alternatively activated macrophages derived from monocytes and tissue macrophages are phenotypically and functionally distinct. *Blood* 2014;123:e110–e122.